Tomás Bauleth Quinta Ferreira Ramos

EpCAM-Conjugated Porous Silicon Nanoparticles for Targeted Cancer Chemoimmunotherapy

Monografia realizada no âmbito da unidade Estágio Curricular do Mestrado Integrado em Ciências Farmacêuticas, orientada pelo Professor Doutor João Nuno Sereno Almeida Moreira e apresentada à Faculdade de Farmácia da Universidade de Coimbra

Setembro 2014

· U C ·

UNIVERSIDADE DE COIMBRA

Eu, *Tomás Bauleth Quinta Ferreira Ramos*, estudante do Mestrado Integrado em Ciências Farmacêuticas, com o nº *2009010447*, declaro assumir toda a responsabilidade pelo conteúdo da Monografia apresentada à Faculdade de Farmácia da Universidade de Coimbra, no âmbito da unidade Estágio Curricular. Mais declaro que este é um trabalho original e que toda e qualquer afirmação ou expressão, por mim utilizada, está referenciada na Bibliografia desta Monografia, segundo os critérios bibliográficos legalmente estabelecidos, salvaguardando sempre os Direitos de Autor, à exceção das minhas opiniões pessoais.

Coimbra, --------- de--------- de 2014.

Assinatura do Aluno

(Tomás Bauleth Quinta Ferreira Ramos)

Assinatura do Aluno

(Tomás Bauleth Quinta Ferreira Ramos)

Assinatura do Tutor

(Prof. Dr. João Nuno Moreira)

Coimbra, _____ de Setembro de 2014

Acknowledgements

I would like to express my sincere gratitude to my supervisors in Helsinki, Dr. Hélder Santos and Dr. Ali Shabazzi. Thanks for letting me be part of Hélder's group, for the continuous support, patience, motivation and knowledge. Without their guidance I could not have done it.

My sincere thanks also go to my supervisor in Portugal, Dr. João Nuno Moreira for the guidance and support in my work.

Also to all my labmates in Hélder's group, for all the help and support with the work.

To my friends, Ricardo Rosa, Sami Svanback, Patrick Almeida, Sérgio Almeida, Stijn Van Landeghem and Sylvie Langeraert, thank you for all the friendship you have shown, and for making this a most spectacular experience.

I want to thank as well to the University of Coimbra for the scholarship that allowed me to go to Helsinki and to the University of Helsinki for the opportunity.

To Sofia and all my Portuguese friends thanks for all you have done for me.

Last but not least, I would like to thank my family for all the love and support throughout my all life that made me who I am, and allowed me to get this far. I could never ask for more than you gave me.

Table of Contents

Abbreviations

Ab – Antibody

ADCC – Antibody-dependent cellular cytotoxicity

APCs – Antigen Presenting Cells

CDC – Complement-Dependent Cytotoxicity

CLSM – Confocal laser scanning microscopy

DLS – Dynamic Light Scattering

DMEM – Dulbecco's Modified Eagle Medium

EDC – 1-ethyl-3-(3-dimethylaminopropyl)carbodiimide

EPR – Enhanced Permeation and Retention

FBS – Fetal Bovine Serum

FITC – Fluorescein Isothiocyanate

FTIR – Fourier Transform Infrared Spectrometer

HBSS – Hank´s Balanced Salt Solution

HEPES – HBSS–4-(2-hydroxyethyl)-1-piperazineethanesulfonic acid

mAbs – Monoclonal Antibodies

MES – 2-(N-morpholino)ethanesulfonic acid

NHS – N-hydroxysuccinimide

NPs – Nanoparticles

PBS – Phosphate Buffer Saline

PSi – Porous silicon

RPMI-1640 – Roswell Park Memorial Institute Medium

TCPSi – Thermally Carbonized PSi

TEM – Transmission Electron Miscroscopy

THCPSi – Thermal Hydrocarbonized PSi

TOPSi – Thermal Oxidized PSi

UnTHCPSi – Undecylenic acid Thermally Hydrocarbonized PSi

Abstract

Porous silicon (PSi) nanoparticles (NPs) are known for being high efficient drug delivery vehicles for poorly water-soluble drugs, e.g. anticancer agents. However, bare NPs lack efficiency as they do not specifically target cancer cells, thus not avoiding interaction with healthy cells.

In this work, sorafenib, an anticancer agent, loaded undecylenic acid thermally hydrocarbonized PSi (UnTHCPSi) NPs were successfully biofunctionalized with anti-EpCAM antibody (Ab), to target CD326 receptor overexpressing cells in order to enhance intracellular uptake and avoid interaction with healthy cells. In addition to the improvement of sorafenib dissolution in plasma by the UnTHCPSi NPs, these NPs have also shown low cytotoxicity, resulting in enhanced biocompatibility. The biofunctionalization with the antibody have led to a significant increase in cellular uptake by MCF-7 breast cancer cells (CD326 overexpressing cells) when compared with the control, MDA-MB-231 breast cancer cells (do not express CD326). Besides, the enhanced cellular uptake has resulted in a significant increase in the *in vitro* antiproliferation effect. The results were confirmed by TEM, flow cytometry and confocal microscopy.

Our achievements demonstrated the potential of the anti-EpCAM conjugated UnTHCPSi NPs to enhance anticancer therapy by improving drug release, intracellular uptake and active targeting.

Resumo

Nanoparticulas (NPs) porosas de silício (PSi) são veículos altamente eficientes para entrega de fármacos pouco hidrossolúveis, como por exemplo, fármacos anticancerígenos. Contudo, este tipo de NPs têm falta de eficácia se não sofrerem funcionalização. Isto deve-se à sua baixa especificidade para células cancerígenas, o que leva a interacções indesejáveis com as células saudáveis.

Neste trabalho, o fármaco anticancerígeno sorafenib foi incorporado, com sucesso, em NPs porosas de silício tratadas com ácido undecilénico (UnTHCPSi) e posteriormente biofuncionalizadas com o anticorpo anti-EpCAM. Além de promoverem a dissolução do sorafenib no plasma, estas NPs possuem baixa citotoxicidade, resultando numa maior biocompatibilidade. A biofuncionalização com o anticorpo levou a um aumento significativo do *uptake* pelas células mamárias cancerígenas MCF-7 (sobreexpressam o receptor CD326),

quando comparadas com as MDA-MB-231 (não expressam o receptor e por isso são consideradas como grupo controlo). Este aumento resultou num maior efeito antiproliferativo, in vitro.

Os resultados, confirmados por microscopia electrónica de transmissão, citometria de fluxo e microscopia confocal, demonstraram que as UnTHCPSi NPs conjugadas com o anticorpo anti-EpCAM, têm capacidade para melhorar a terapia anticancerígena, através de um aperfeiçoamento da libertação do fármaco, *uptake* intracelular e *targeting*.

1. Introduction

Cancer is one of the major health issues in the world, remaining the leading cause of death worldwide.[1] Breast cancer represents the second most common cancer, the fifth most lethal, and are most frequent in women.[2] In 2012, according to the World Health Organization, cancer caused nearly 8.2 million deaths (522.000 by breast cancer)[3] and is estimated to lead to 13.1 million deaths (770.000 by breast cancer) in 2030.[4] Despite intensive research in the cancer area, current therapies (e.g., radiotherapy and chemotherapy) are not very effective yet. The poor bioavailability and poor pharmacokinetics of the chemotherapeutic, as well as the physiological barriers are some key reasons for cancer treatment failure.[5, 6] Therefore, there is an ever increase need to find new therapeutic targets and ways to overcome this failure. Recently, there have been some advances in areas such as genomics, immunotherapy, and nanotechnology which, together with advances in cancer biology, can lead to new methods to treat cancer.[7]

Immunotherapy has already shown a high potential and a major role in the fight against cancer.[8] This method consists of using the immune system to fight and destroy the cancer cells. The use of synthetic particles that mimic antigen presenting cells (APCs) to induce T-cell activation, differentiation and also help to stimulate B cells into secreting antibodies,[9] has gained great attention within the scientific community. Another strategy is to use monoclonal antibodies (mAbs), which have different functions such as activation of the proteolytic cascade, that leads to the opening of pores in the membrane of target cells, antibody-dependent cellular cytotoxicity (ADCC), complement-dependent cytotoxicity (CDC) and targeting.[10] Their major advantage is their specificity to the target (antigen) site, by avoiding interaction with healthy cells, hence minimizing the side effects. However, mAbs also have disadvantages like the poor ability to penetrate tumors.[11, 12] Subsequently, to

achieve maximum effectiveness, mAbs should have long half-life, ability to penetrate the tumor and the target antigen should be tumor specific to minimize nonspecific toxicity.[13]

Tumors have a natural resistance to the immune system as they are developed from the body's own cells, thus not recognized as foreign cells and a potential threat. Furthermore, the immunological response may not be strong enough to destroy the cancer cells in this case.[14] In addition, tumors usually recruit and co-opt immunosuppressive cells such as regulatory T-cells and tumor associated macrophages that will secrete tumor growth factors. In order to overcome these drawbacks there is a demand for combined targeted chemotherapy and immunotherapy. Nanoparticles can be very useful in combination therapies, owing to their physicochemical characteristics the ability to regulate their biodistribution,[9] overcoming problems related to poor drug pharmacokinetic profiles and their lack of tumor specificity.[15]

Nanomedicine is a branch of nanotechnology that holds a great promise for cancer therapy. By the Lux Research, in 2006 were spent $12.4 billion worldwide in research and development. It is estimated that this year, 2014, the value will rise to $2.6 trillion, or about 15% of the total global output in manufactured goods.[16] The used biomaterials must be designed to achieve certain physiological responses, such as pH-sensitivity, biodegradability, and also mechanical properties such as size, surface area, and porosity.[17] In this context, mesoporous materials are an excellent choice due to their physicochemical characteristics. Mesoporous materials have a large surface area (>700 m2/g)[18] that allows drug adsorption, surface functionalization and enhancement of drug dissolution rates.[19] They also have large pore volume (>0,9 cm3/g)[20] which can easily be tailored (pore diameters 2–50 nm) to act as reservoirs for different payloads.[18] As the pores size is not much larger than the drug molecules, the drug stays in its amorphous form when loaded inside the mesoporous, and thus, increasing its solubility and permeability across the cells membranes.[19] Furthermore, the stability and rigid framework of mesoporous materials make them resistant to pH, mechanical stress and fast degradation.

PSi are mesoporous materials fabricated by a top-down approach from Si wafers via electrochemical etching to produce controlled nanostructures.[21] According to the needs, the PSi surface can be prepared as hydrophobic or hydrophilic, with negative or positive charge, depending on the applied method: thermal oxidation (SiO2) of PSi (TOPSi) – hydrophilic and negative surface charge; thermal carbonization (SixCy) of PSi (TCPSi) – hydrophilic and negative surface charge; and thermal hydrocarbonization (Si-C-Hx) of PSi

(THCPSi) – hydrophobic and slightly positive surface charge. The PSi surface can be further functionalized to enhance biofunctionalization[20] by carboxylation (–COOH)[22, 23] and amino-grafting (–NH2).[24] PSi are also chemical inert, thermally stable,[20] biocompatible,[25] biodegradable, and the degradation product is orthosilicic acid [Si(OH)4], a nontoxic compound.[26]

Due to their characteristics, PSi nanoparticles can revolutionize the biomedical field as a controlled drug delivery, diagnosis, imaging, and targeting platform.[27, 28] For imaging/diagnosis purposes, PSi nanoparticles exhibit intrinsic luminescence,[29] and thus can be imaged using several techniques, such as near-infra-red imaging,[30] and radiolabelled with fluorine-18,[20] which allows imaging by positron emission tomography.[31]

Targeting can be achieved using passive and active strategies. Passive targeting relies on the tumor characteristics such as hyperpermeable and leaky microvasculature as well as limited lymphatic drainage.[32] The particles can be designed so that they can accumulate due to their size and extravasation within the tumor (at <80 nm the nanoparticles will be cleared away by drainage to the capillary pores)[10] by the so-called enhanced permeation and retention (EPR). However, passive targeting is not cell-specific, leading to a decrease in therapeutic efficacy and induction of drug resistance. In contrast, there is the possibility to conjugate the nanoparticles with different target moieties such as folic acid, aptamers and antibodies, which are specific to different epitopes or receptors that are exclusive or overexpressed in the tumoral cells. This conjugation leads to a further specific targeting, reducing the interaction with healthy cells, hence minimizing the side effects.[33] Antibody-conjugated PSi nanoparticles loaded with camptothecin (a hydrophobic anticancer drug) and functionalized with MLR2, mAb528 and Rituximab antibodies have been shown to be efficient to target cancer cells and were lethal without interacting with cells that do not express the tumor receptors.[15] Other studies have shown that PSi-conjugated with CD40 mAb besides promoting the uptake due to engagement to the receptors also amplified the antibody's activation potency with regard to B cells. [34, 35]

Thus, one possible new way to treat cancer is to use PSi nanoparticles loaded with anticancer drugs, and conjugated with mAbs, in order to target them to cancer cells and also to trigger the immune system.

The aim of this study was to use UnTHCPSi nanoparticles loaded with sorafenib (an anticancer drug)[36] and functionalized with anti-EPCAM (anti CD326) antibody to target breast cancer cells that overexpress the CD326 antigen. The chosen cells were MCF-7

breast cancer cells, which overexpress CD326 and also MDA-MB-231breast cancer cells to serve as control, as they do not overexpress this particular antigen. Therefore, the idea was to demonstrate that UnTHCPSi conjugated nanoparticles (NPs) can improve the therapeutic effect of the anticancer agent by improving the solubility of sorafenib and enhancing the targeting capacity delivering the drug to the tumor cells.

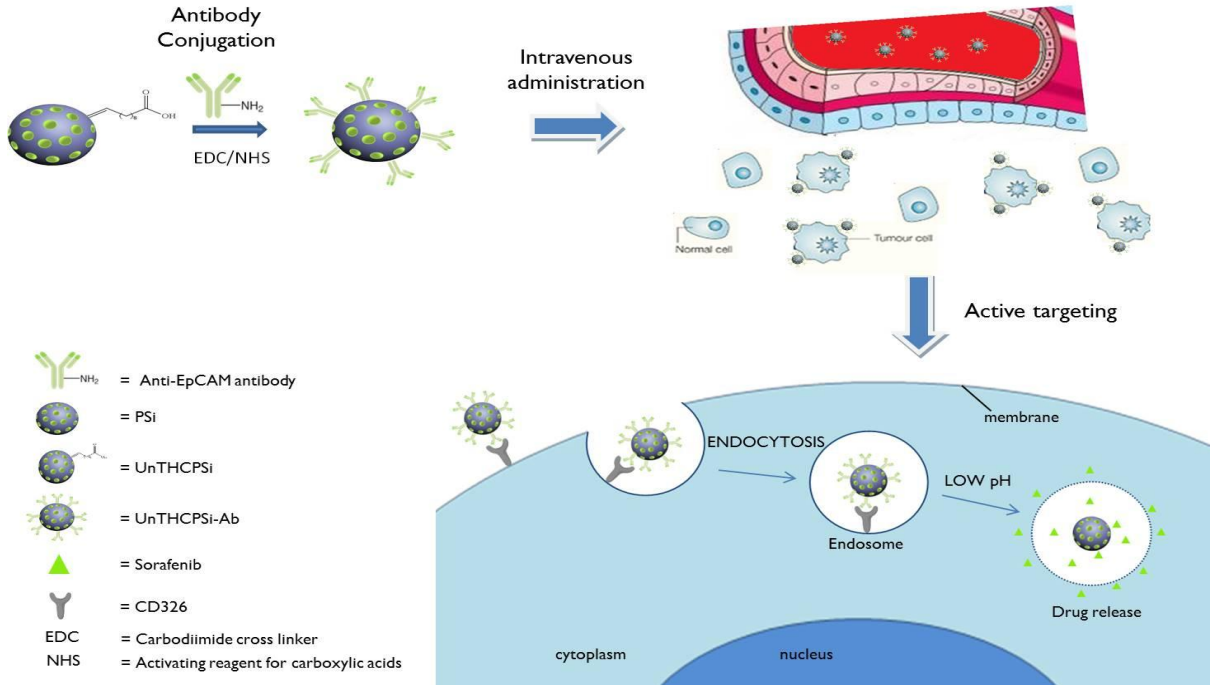

Figure 1. *Chemoimmunotherapy of breast cancer cells and promoted receptor-mediated endocytosis using anti-EpCAM antibody conjugated UnTHCPSi nanoparticles loaded with Sorafenib.*

2. Materials and Methods

2.1. Preparation and characterization of PSi NPs

Briefly, free-standing multilayer PSi films were electrochemically anodized from monocrystalline, boron doped p+ Si ⟨100⟩ wafers with a resistivity of 0.01–0.02 Ω.cm using a 1:1 (v/v) hydrofluoric acid (38%)-ethanol electrolyte.[18, 37] The multilayer structure was formed by applying a repeating pulsed low/high etching profile, designed to create fracture planes on the Si wafers at desired intervals. The multilayer film was then lifted off from the substrate by increasing the etching current abruptly to the electropolishing region. Fresh PSi multilayer films were then exposed to N_2 flow (1 L/min) for at least 30 min in order to remove residual moisture and oxygen. Afterwards, acetylene (C_2H_2) flow (1 L/min) was

added to the N_2 flow for 15 min at RT followed by a heat treatment for 15 min at 500 °C under the 1:1 (v/v) N_2/ C_2H_2 flow. Then, wet ball milling was carried out in 1-decene to minimize the surface oxidation, and the produced THCPSi films were allowed to cool down to RT under N2 flow.[38] UnTHCPSi NPs were obtained from THCPSi films by immersing them into undecylenic acid for 16 h at 120 °C followed by milling in ethanol.[22]

The average particle size and average zeta-potential measurements of UnTHCPSi particles were determined by dynamic light scattering (DLS) using a Zetasizer Nano ZS instrument (Malvern Instruments Ltd., UK) at 25 °C. The particles were suspended in Mili-Q water.

To examine the chemical structure of the UnTHCPSi NPs and Ab conjugated UnTHCPSi, Fourier transform infrared spectrometer (FTIR) was used. Prior to the analysis, the NPs were dried at room temperature overnight. The transmittance spectra were recorded between 4000 and 650 cm-1 with a 4 cm-1 resolution, using OPUS 5.5 software in Vertex 70 FTIR spectrometer (Bruker Optics, USA).

The structural properties of the UnTHCPSi NPs were characterized by N2 sorption with Tristar 3000 equipment (Micromeritics Inc., USA) at −196 °C. The specific surface area was determined by means of the Brunauer-Emmett-Teller theory.[39] The pore volume was obtained from the total adsorbed amount at a relative pressure p/p0=0.97 and the average pore diameter were calculated assuming the pores as cylindrical, using the values of total pore volume and specific surface area. These experiments were conducted by the Laboratory of Industrial Physics, University of Turku, Finland.

2.2. Conjugation of Ab to PSi NPs

To conjugate the NPs with the anti-EpCAM antibody (Sigma-Aldrich, Finland), 200 µg of the UnTHCPSi were suspended in 1 mL of 2-(N-morpholino)ethanesulfonic acid (MES) 10mM (pH 5.5). 2 µL of 1-ethyl-3-(3-dimethylaminopropyl)carbodiimide (EDC) and 1 µg of N-hydroxysuccinimide (NHS) were then added. The solution was then stirred for 2 h in the dark to activate carboxyl groups of the NPs. The pH was adjusted to 6.5 before adding the Ab and stirring for 30 min in dark. Finally, the sample was centrifuged at 13200 rpm for 5 min, the supernatant removed, and the Ab conjugated NPs were dispersed in phosphate buffer saline (PBS) solution (pH 7.4).

2.3. Drug loading and release

Sorafenib-loaded UnTHCPSi NPs were prepared by immersing 100 µg of the NPs in 2 ml of the drug solution (0.5 mg/ml) in acetone, and then stirring for 2h at room temperature. Next, the excess amount of the drug was removed by ultracentrifugation at 15000 rpm for 5 min (Kendro/Sorvall Ultraspeed Centrifuge, Artisan Scientific Corporation, Champaign, IL), followed by three washes with MiliQ water. The recovered NPs were used for further functionalization with the EpCAM antibody. To determine drug loading degree, 100 µg of the sorafenib-loaded UnTHCPSi NPs nanoparticles were immersed in 1 mL of the acetone under vigorous stirring for 60 min. The suspensions were then centrifuged at 15000 rpm for 5 min and the supernatant used for the detection of sorafenib using a reverse-phase HPLC (Agilent 1260, Agilent Technologies, USA). The chromatographic separation was achieved using a Zorbax Eclipse XDB-C8 (4.6×150 mm, 5 µm) column. The mobile phase was composed of trifluoroacetic acid (pH 2) and acetone at a ratio 42:58 (v/v %) with 1.0 mL/min flow rate and UV-detector set at wavelength of 254 nm.

In vitro drug release profile of the sorafenib loaded NPs was determined by redispersing 200 µg of the loaded NPs in 50 mL of plasma at 37 °C and a stirring speed of 150 rpm. 200 µL of the release medium solution was withdrawn at predetermined time points, and replaced with equal volume of the corresponding fresh pre-warmed medium to retain a constant volume of the release medium. After sampling, the aliquots were centrifuged for 3 min at 15000 rpm and the amount of sorafenib was analyzed by HPLC as described in the loading section. For drug release assessment in the plasma, the supernatant of centrifuged samples was mixed with acetone at 1:1 ratio and centrifuged to precipitate and separate plasma proteins. All measurements were performed in triplicate.

2.4. Cell cultures

MCF-7 breast cancer cells were cultured in high glucose (4.5 g/L) Dulbecco's modified Eagle medium (DMEM) containing 10% FBS (Fetal Bovine Serum), 1% L-glutamine, 100 IU/mL penicillin and 100 mg/mL streptomycin, and 1% nonessential amino acids (all from HyClone, USA). MDA-MB-231 breast cancer cells were cultured in RPMI-1640 (Roswell Park Memorial Institute Medium) (HyClone, USA) with the same supplement as for MCF-7 cells. All the cell lines were maintained in a humidified atmosphere (95% relative humidity) with an atmosphere of 5% CO2 at 37 °C (BB 16 gas incubator, Heraeus Instruments GmbH, Germany). The medium was routinely changed every 3 days, and for passaging and prior to

each test, the cells were harvested with 0.25% (v/v) trypsin-ethylenediamine tetraacetic acid–PBS. Trypsin 2.5% was purchased from EuroClone S.p.A. (Italy) and Dulbecco's PBS (10×) was purchased from Gibco® (Carlsbad, USA). The cell lines were obtained from American Type Culture Collection and cultured in 75 cm2 culture flasks (Corning Inc. Life Sciences, USA).

2.5. Cell viability and proliferation

Typically, 100 µL of the cell suspensions with the concentration of 2×10^5 cells/mL in the cell media were seeded in 96-well plates and allowed to attach overnight. Thereafter, the cell media was removed and replaced with 100 µL of the NPs at concentrations of 5, 10, 25, 50, 100 and 200 µg/mL. After 24 and 48 h incubation at 37 °C, 100 µL of the reagent assay (CellTiter-Glo® Luminescent Cell Viability Assay, Promega, USA) was added to each well as described elsewhere.[40] The luminescence of the wells was measured using a Varioskan Flash (Thermo Fisher Scientific Inc., USA). Negative [HBSS (Hank´s Balanced Salt Solution) buffer solution] and positive (1% Triton X-100) control wells were also used and treated similarly as described above. The viability of the negative control was taken as 100%. The results are shown as the average of at least three independent measurements. The cell proliferation effects of the free sorafenib and sorafenib-loaded PSi NPs were also performed using the same procedures as described above.

2.6. Confocal Laser Scanning Microscopy (CLSM)

For confocal microscope observations, a density of 5×104 cells/per well of MCF-7 and MDA-MB-231 cells were seeded in Lab-Tek® chamber slides (Thermo Fisher Scientific, USA) with 200 µL of DMEM and RMPI-1640, respectively, and leaved overnight to attach. The medium was removed and 200 µL of fluorescein isothiocyanate (FITC)-labeled pure NPs and Ab-conjugated (50 µg/mL) in the medium, added to each chamber and incubated for 6 h at 37 °C. The cells were then rinsed 3 times with HBSS–4-(2-hydroxyethyl)-1-piperazineethanesulfonic acid (HEPES) pH7.4 purchased from Gibco® (Carlsbad, CA, USA) and Sigma-Aldrich (Finland), respectively, to remove the particles. Afterwards, the cells were washed once with HBSS-HEPES and incubated with CellMask® (3 µg/mL; Invitrogen, USA) for 3 min at 37 °C, in order to stain the cell plasma membrane. To remove the CellMask®, the cells were rinsed 3 times with HBSS-HEPES. Finally, the cells were fixed with 2,5%

glutaraldehyde for 20 min at 37 °C, and washed twice with buffer. The confocal images were taken using a confocal microscope Leica SPS II HCS A (Germany).

2.7. Transmission Electron Miscroscopy (TEM)

The cellular uptake of the NPs by MCF-7 and MDA-MB-231 breast cancer cells was evaluated by TEM. About 10^5 cells/well of MCF-7 cells in DMEM and MDA-MB-231 cells in RPMI-1640, were seeded in 24-well plates (Corning Inc. Life Sciences, USA) with 13 mm round shape coverslips in the bottom, and allowed to attach overnight. The culture media was then removed and 25 μg of the NPs, conjugated and unconjugated with the Ab in suspension were added to each well, followed by 6 h incubation at 37 °C. The NP suspensions were then removed and the cells washed twice with HBSS–HEPES. 2.5% glutaraldehyde in 0.1m PBS solution (pH7.4) was added to each well to fix the cells for 1 h at room temperature. Afterwards, the wells were washed twice with HBSS–HEPES (pH7.4), sodium cacodylate buffer (NaCac) and post-fixed with 1% osmium tetroxide in 0.1 M NaCac buffer (pH 7.4). A series of 30–100% ethanol was added for 10 min to dehydrate the cells prior to embed them in epoxy resin. Lastly, ultrathin sections (60 nm) of the embedded samples were cut parallel to the coverslip prior to stain with uranyl acetate and lead citrate, and observed by Jeol JEM-1400 microscope (Jeol Ltd., Tokyo, Japan).

2.8. Flow cytometry

About 7×105 cells/well MCF-7 and MDA-MB-231 cells were seeded in 6-well plates (Corning Inc. Life Sciences, USA) and incubated at 37 °C overnight. The cells were again incubated for 6 h with FITC-labeled NPs (50 μg/mL), after being washed with HBSS–HEPES (pH 7.4). The cells were detached with trypsin–PBS–EDTA, washed three times with HBSS–HEPES and centrifuged for 3 min at 500 rpm. Then, 2.5% glutaraldehyde in PBS was added for 30 min to fix the cells and the samples were re-suspended with 700 μL of HBSS–HEPES (pH 7.4). The data was collected using a LSR II flow cytometer (BD Biosciences, USA) with a laser excitation wavelength of 488 nm and analyzed with Flowjo 7.6 software (Tree Star, Ashland, OR, USA). In order to study the specific binding of the nanoparticles to CD326 receptors, both cell lines were exposed to pure anti-EpCAM Ab and UnTHCPSi–Ab and the cellular interaction was evaluated after 3 h incubation at 37 °C using flow cytometry.

3. Results and Discussion

3.1. Preparation, characterization and functionalization of PSi NPs

The mean particle size, measured by DLS was 151± 3.2 nm, making them suitable for targeted anticancer therapy, where the size should be between 80nm[10] and 400 nm[41] in order to achieve EPR effect. N2 adsorption/desorption technique showed an average pore volume of 0.70±0.06 cm3/g, average pore diameter of 11.1±0.9 nm, and average surface area of 252±7 m2/g for the UnTHCPSi NPs. By TEM (Fig. 2), it is possible to observe the irregular morphology of the NPs and to see the porous structure that allows drug loading.

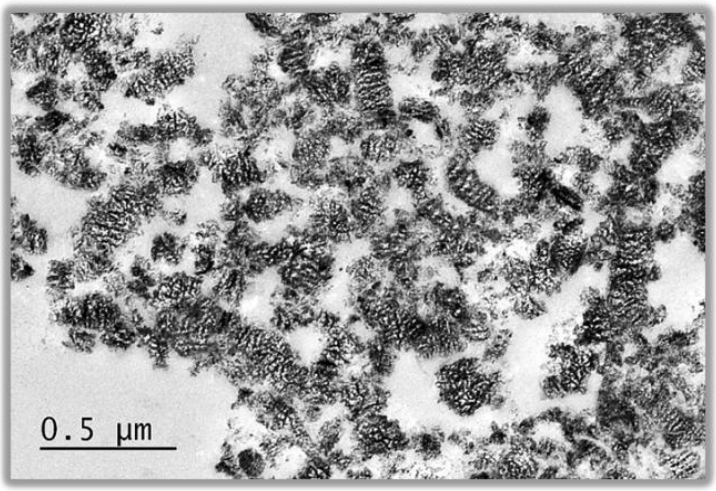

Figure 2. *TEM image of UnTHCPSi NPs.*

The conjugation of the Ab to the UnTHCPSi nanoparticles was made following the steps outlined in the *scheme 1* via the activation of carboxyl groups for reaction with primary amines via amide bond formation in aqueous solution. UnTHCPSi NPs have carboxyl groups on the surface, so, in order to conjugate them with the anti-EpCAM Abs, which have amine groups, first there is the need to activate the carboxyl group from the NPs. To do so, EDC was added to the NP solution at pH 5.5, where the crosslinking is most efficient. Then, NHS was added to further improve the efficiency of the reaction by creating an NHS-ester, more stable than the O-acylsourea intermediate. The used buffer was MES, an aqueous solution without extraneous carboxyls and amines, thereby being suitable for carbodiimide reaction.[42] As the NP:Ab ratio is one of the critical points for proper conjugation, after testing different conditions, 1:10 ratio was selected as the optimum for the preparation of the Ab functionalized NPs.

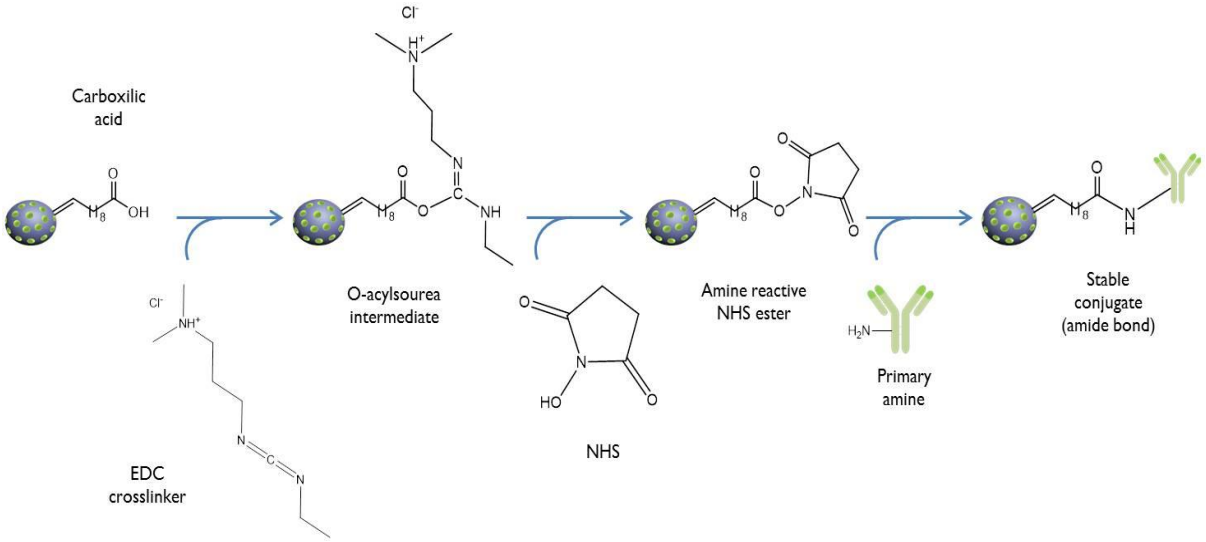

Scheme 1. *Carbodiimide crosslinking reaction using EDC and NHS (not in scale).*

To assess the conjugation successfulness, size, zeta potential (surface charge) and chemical structure of the surface analyses were conducted. All the analyses were done in bare and conjugated nanoparticles as a mean of comparison. After the conjugation, not only the size of the particles increased from 171.3±1.15 to 338±7.54 nm, there was also a change on the surface charge from negative –29.0±0.6 mV to +11.6±1.135 mV. This change can be explained by the presence of Ab on the surface of the UnTHCPSi NPs. The loading of the drug did not affect significantly the size of the particles (173±1.73 nm), however it affected the surface charge as the values changed from –29.0±0.6 mV to –19.2±0.4 mV, indicating a possible interaction between the drug and the particles surface.

Further evaluation of the surface of the particles was done by analyzing the samples with FTIR. The spectra for bare UnTHCPSi NPs (Fig. 3) show bands corresponding to CH stretching, carboxyl C=O stretching, and CH_2 deformation displayed at 2922, 1709, and 1469 cm− 1, respectively. Also, the spectra for the Ab-conjugated UnTHCPSi NPs (Fig. 3) showed a shift to the right, in which the C=O carboxyl band disappeared, and bands for amide I, C=O stretching, and amide II N-H bending and C-N stretching were displayed at 1656 and 1537 cm− 1, respectively. The disappearing of the carboxyl group and appearing of amide group, alongside with the increase of the size and the surface charge change indicates a successful conjugation of Abs to the surface of the NPs.

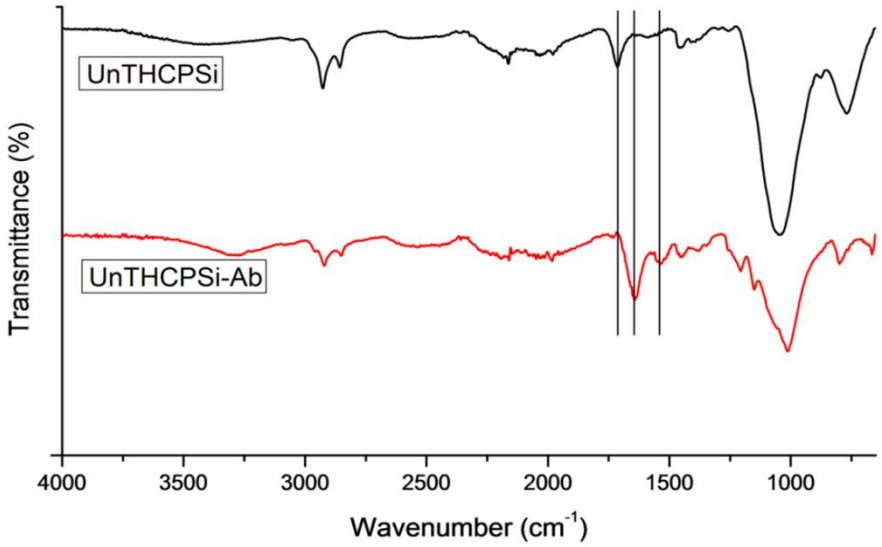

Figure 3. *Characterization by FTIR of the UnTHCPSi and Anti-EpCAM-conjugated UnTHCPSi NPs surface. The shift to the right of the peak around 1700 cm-1 shows the success of the conjugation due to the disappearance of the carboxyl group peak and appearance of the amide peak.*

3.2. Cell viability

There are several aspects that influence the cytotoxicity of the NPs such as size, surface chemical composition and charge.[43, 44] In order to check the possibility to use anti-EpCAM conjugated UnTHCPSi NPs as a drug delivery vehicle, the in vitro cytotoxicity of the NPs was tested. The cell viability assay was performed in two types of breast cancer cells, MCF-7 and MDA-MB-231, using both Ab-conjugated and bare UnTHCPSi NPs. The experiment consisted in the incubation of the cells, for 24 and 48h, with different concentrations of the NPs followed by the assessment of their ATP activity. The ATP activity is directly proportional to the number of viable cells,[45] thereby allowing to calculate the cytotoxicity by comparison with a negative control.

As shown in Fig. 4, for MCF-7 breast cancer cells, at both 24 (Fig. 4A) and 48h (Fig. 4B) there was almost no toxicity for conjugated and bare NPs until concentrations of 100 µg/mL. More than 90% of the cells were viable and these non-toxicity levels can be hypothetically explained due to the low stability and aggregation in aqueous media, resulting in low cellular interaction and reduced cytotoxicity. However, for concentrations above 100 µg/mL (e.g., 200 µg/mL), there was a significant decrease in the cell viability to values between 40–60%. In MDA-MB-231 cell line, in the first 24h (Fig. 4C), there was a small decrease in the viability

concentration dependant until values of 100 µg/mL. However, for higher values (200 µg/mL) the decrease was most significant. Thereby, the results showed that the PSi NPs have biocompatibility and are safe to use for drug delivery applications with concentrations until 100 µg/mL in the tested conditions.

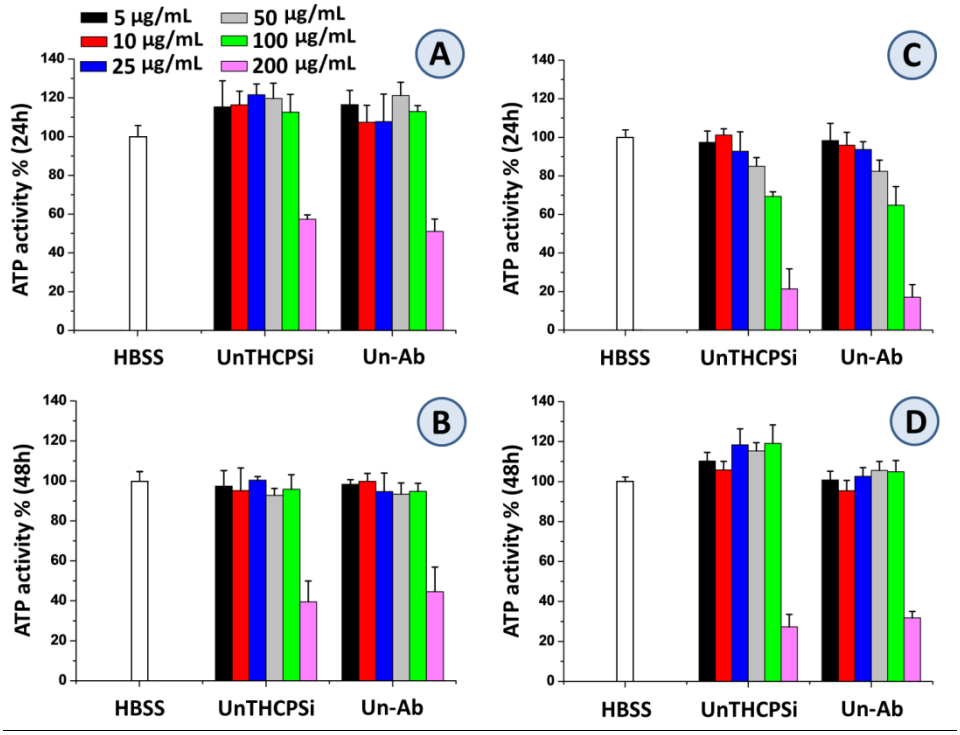

Figure 4. *ATP-based in vitro cytotoxicity test of UnTHCPSi and UnTHCPSi-Ab (Un-Ab), after incubation of different concentrations of NPs with MCF-7 cells for 24 (A) and 48 h (B), and with MDA-MB-231 cells for 24 (C) and 48 h (D) at 37 °C, using CellTitel-Glo® luminescent assay. Error bars represent mean ±s.d. (n ≥ 3).*

3.3. Drug loading and release studies

Most of anticancer drugs lack water solubility,[5] becoming a huge problem in the administration. Loading the drug into NPs is one way to overcome this, as they can improve its solubility. To investigate the possibility to do it with the nanoparticles in study, firstly, sorafenib was loaded into UnTHCPSi and UnTHCPSi-Ab NPs, followed by evaluation of drug release over time.

Sorafenib was successfully loaded into the NPs, with loading degrees of 11.91 w-%. As this system is to be administered intravenously, the drug release evaluation was made in human plasma at pH 7.4, mimicking the bloodstream or extracellular fluids within normal tissues. Fig. 5 confirm the lack of water solubility of sorafenib,[46] as only around 15% of the

drug was dissolved in human plasma. The use of PSi NPs, as expected, led to a significant increase in the solubility of the anticancer agent. In fact, in the first 25 min 40% of the drug was already dissolved and the value was maintained around that percentage until 4h of testing, time where the values started to increase reaching 50% of drug release at ca. 6 h. However, when the NPs were conjugated with the Ab, there was a decrease in the release when compared with bare NPs, to values around 25% release, which were still higher than the ones from free sorafenib. This is possibly explained due to physical or chemical interactions between the drug and the surface of the NPs. As the drug was loaded before Ab conjugation, it is possible that the Ab blocks some of the porous of the NPs, thereby not allowing the drug to be fully released from the pores of the NPs. Chemical interactions between the drug and the Ab are also likely to take place as the drug is highly negatively charged and the anti-EpCAM Ab has several amine groups, which can lead to a reaction between these groups, leading to electrostatic interactions that will slow down the drug release.

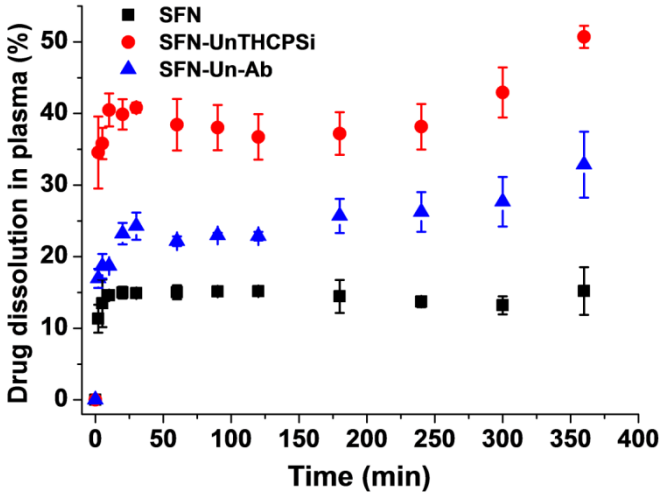

Figure 5. *Drug dissolution profile in human plasma of pure sorafenib (black square), bare UnTHCPSi NPs loaded with the drug (red circles), and Un-Ab NPs loaded with the drug.*

3.4. Targeting CD326 receptor overexpressed in breast cancer cells

As previously explained, PSi NPs used as a drug delivery system can help to surpass the difficulties of delivering cytostatic drugs to the tumor tissue;[15] however, the size, surface charge, and chemical composition of the NPs influence the interaction with the cells.[43, 44] With the conjugation of certain moieties, like a specific Ab, there can be an improvement in

the intracellular uptake.[34] Therefore, there was a need to evaluate the capacity of anti-EpCAM conjugated UnTHCPSi to target breast cancer cells and its effects in cellular uptake. To do it, TEM, flow cytometry and confocal microscopy analyses were performed.

In the first place, the antigen expression was assessed by flow cytometry (Fig. 6) by applying FITC-labelled anti-EpCAM Ab to MCF-7 and MDA-MB-231 cell lines. The results proved that MCF-7 breast cancer cells, unlike MDA-MB-231 cells, overexpress the CD326 antigen. This makes both cell lines suitable to test the effect of the anti-EpCAM Ab in targeting, as well as well as to study the interactions with the cells surface and intracellular uptake.

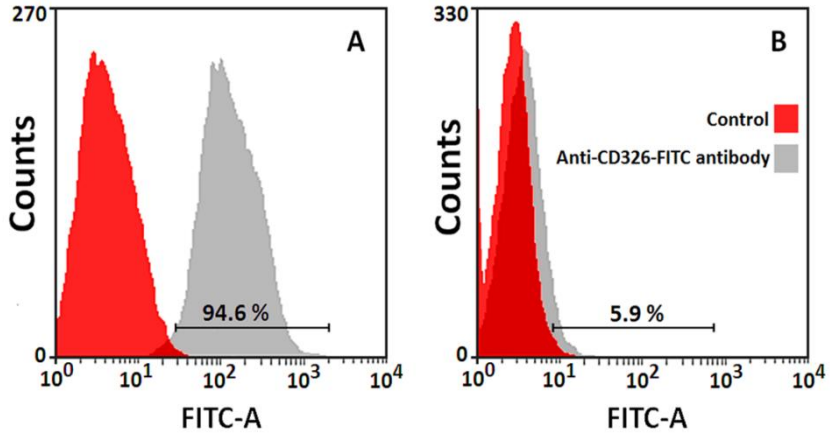

Figure 6. *Flow cytometry imaging to show CD326 expression on the surface of MCF-7 (A) and MDA-MB-231 (B) breast cancer cells.*

Bare and Ab-conjugated UnTHCPSi NPs were incubated for 6 h at 37 °C, with both cell lines, and analysed by TEM. As it is shown in Fig. 7, there was almost no interaction between the bare NPs and both type of cells (Fig. 7A and 7C). It has happened probably due to instant aggregation of the NPs and, thereby, to a reduction in cellular interaction leading to a significant reduction in the cellular uptake. In MDA-MB-231 cells, the difference between the conjugated (Fig. 7D) and bare NPs (Fig. 7A) was not pronounced since this type of cells do not express the CD326 receptor; however, the higher uptake with the conjugated NPs is in agreement with other reports in the literature that show that NPs positive surface charge is beneficial for the non-specific cell internalization.[47, 48] In contrast, for the MCF-7 cells treated with Ab-conjugated NPs , there were a lot of particles attached to the cell membrane and also localized inside the cells (Fig. 7B) (Fig. 7A), confirming that

anti-EpCAM Ab has the ability to enhance the targeting effect and the cellular uptake through CD326 receptor leading to a more efficient therapy.

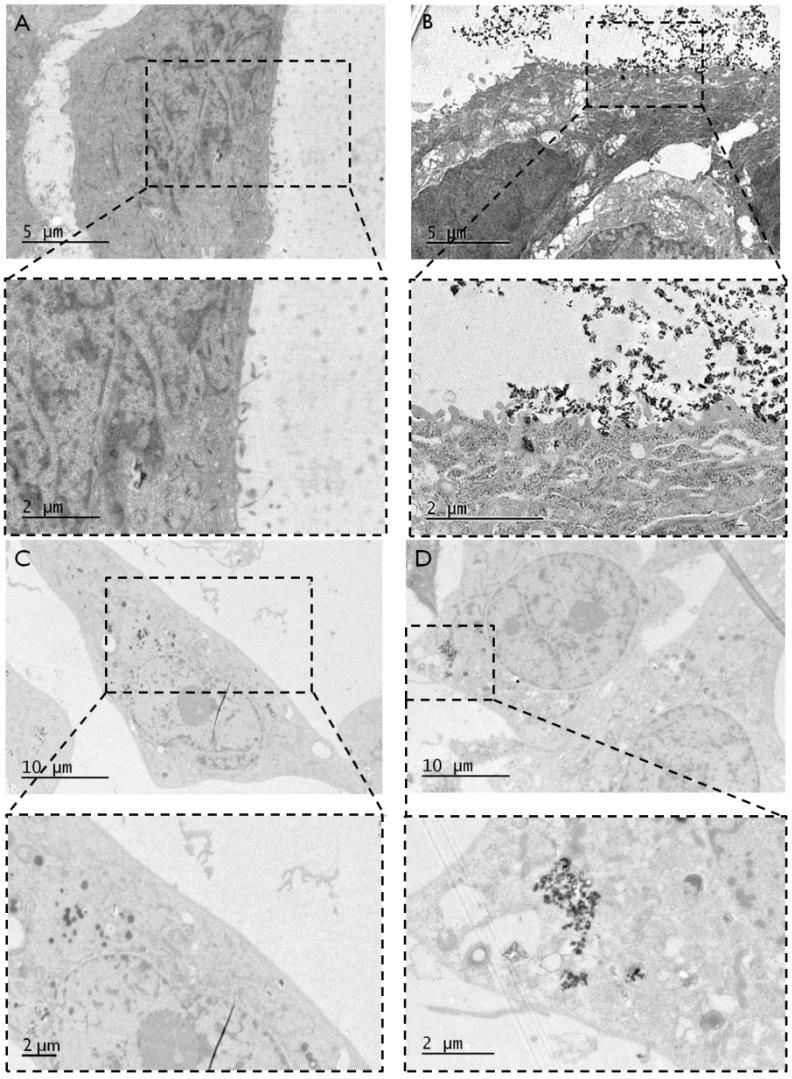

Figure 7. *Targeting and intracellular uptake of UnTHCPSi-Ab and UnTHCPSi NPs. TEM images of MCF-7 and MDA-MB-231 cells incubated with bare and conjugated NPs. (A) UnTHCPSi and (B) UnTHCPSi-Ab with MCF-7 cells. (C) UnTHCPSi and (D) UnTHCPSi-Ab with 231 cells (scale bars are from 10, 5 and 2 µm). Zoom of the TEM images are in the dashed-lines.*

Similar to the TEM results, the confocal fluorescence microscopy analysis (Fig. 8 A and B) have also shown a negligible uptake of the bare UnTHCPSi NPs in both cell lines. When the particles were conjugated with the Ab, it was possible to observe a clear co-localization of the NPs and the surface of the cells, confirmed by the green fluorescence, and an increase in cellular uptake through the overlapped yellow color (Fig. 8). The explanation for this event in MCF-7 cells (Fig. 8A) is possibly due to the overexpression of the CD326 antigen in

this type of cells, whereas with the MDA-MB-231 cells (Fig. 8B) it was probably due to the more positive charge of the NPs' surface, as previously explained.

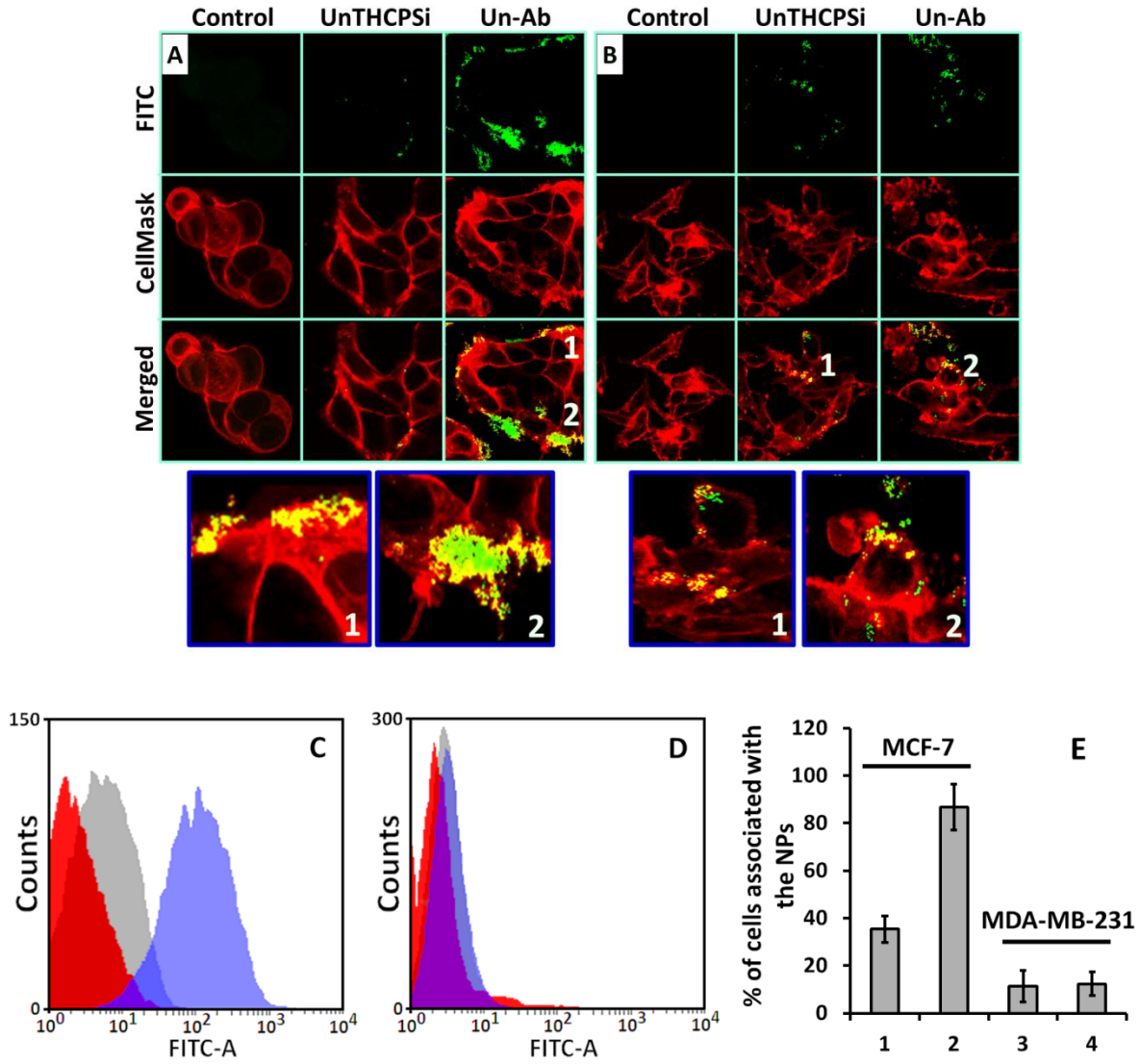

Figure 8. *Confocal fluorescence microscopy images of MCF-7 cells (A) and MDA-MB-231 cells (B) incubated for 6 h at 37 ºC with UnTHCPSi and UnTHCPSi-Ab NPs. The NPs were FITC-labelled (green colour), and the cell membrane was stained with CellMask™ (red colour). (1) and (2) are amplifications of the images showing the interaction between the particles and the surface of the cells (green dots) and the cellular uptake (yellow dots). Flow cytometry qualitative analysis of MCF-7 cells (C) and MDA-MB-231 cells (D) incubated with control (red), Un-Ab (blue), and with Un-Ab, after subjected to competition (grey). Flow cytometry and quantitative determination (E) of the internalization of Un-Ab NPs with (1 and 3) and without competition (2 and 4).*

To be sure that CD326 antigen had a major role in cellular uptake, a competition experiment was conducted. In this experiment, both cell lines were incubated first with free anti-EpCAM Ab and then with the FTIC-labeled UnTHCPSi-Ab, to be analyzed by flow cytometry. As a mean of comparison, cell lines incubated with FTIC-labeled UnTHCPSi-Ab without using free Ab were also tested. And, cells treated with HBSS were considered as control.

The qualitative results (Fig. 8C and 8D) clearly showed that cellular uptake was due to the CD326 antigen on the surface of the cells. For MCF-7 cells (Fig. 8C) there was a big shift to the right of the samples treated with Un-Ab NPs without any previous competition (blue peak) when compared with the ones treated with competition (grey peak). With competition, the CD326 antigens were occupied by free anti-EpCAM Ab, and thus the Un-Ab nanoparticles could not have attached to this specific antigen. The results with MDA-MB-231 cells (Fig. 8D) provided even more evidence, as they do not express the CD326 antigen, and there was no significant difference in the uptake between the cells with or without competition. All of this enforces the idea that cellular uptake is related to the Ab-antigen interaction. In fact, around 90% of the MCF-7 cells were associated with Un-Ab NPs when there was no competition (Fig. 8E-2), but only 38% of the cells were associated with the conjugated NPs with competition (Fig. 8E-1). As expected, for MDA-MB-231, the quantitative results, were the same with or without competition, only around 10% of the cells are associated to the particles.

It is safe to conclude that the expression of CD326 on the surface of the cells is responsible for the targeting effect of anti-EpCAM UnTHCPSi NPs and is the main mechanism for the cellular uptake.

3.5. Cell proliferation

When studying new materials to be used in biomedical applications it is most important to assess their toxicological issues.[49] To test the anti-proliferation effect of bare and Ab-conjugated UnTHCPSi NPs loaded with sorafenib, an ATP-based luminescence cell proliferation assay was conducted in MDA-MB-231 and MCF-7 cell lines. First, the cells were seeded and incubated with sorafenib-loaded Ab-conjugated UnTHCPSi NPs, sorafenib-loaded UnTHCPSi and pure drug at different concentrations to test cell proliferation. Afterwards, the CellTiter-Glo® reagent which generates a luminescent signal proportional to

the live cells was employed, thereby allowing to calculate the percentage of viable cells.[45] The analyses were done at 24 and 48h.

The results in MDA-MB-231 cells (Fig. 9) showed no differences between the conjugated and the bare NPs, neither at 24 h or at 48h. It can be explained due to the fact that this breast cancer cells do not express the CD326 antigen, thereby the anti-EpCAM Ab would not have effect in the targeting and cellular uptake, as previously discussed. In contrast, for MCF-7 breast cancer cells (Fig. 9), the conjugated NPs could inhibit much more efficiently the proliferation of the cells than the bare NPs. This pointed the existence of targeting effect of the conjugated NPs via the CD326 receptor, resulting in receptor-mediated endocytosis, and consequently increasing the internalization of the NPs, leading to a higher percentage of drug release in the MCF-7 cells.

Regarding the pure drug results, they showed higher toxicity levels than the loaded nanoparticles, which could raise the question if the system is more efficient than the pure drug. Yet, this experiment was conducted by the amount of drug loaded inside the particles and not from the released amount. Thus, the previous drug release tests disclaim this conclusion as they showed that there was no complete drug release from the nanoparticles making the concentration of drug affecting the cells in this test much higher for the pure drug rather than for the nanoparticles loaded with the drug.

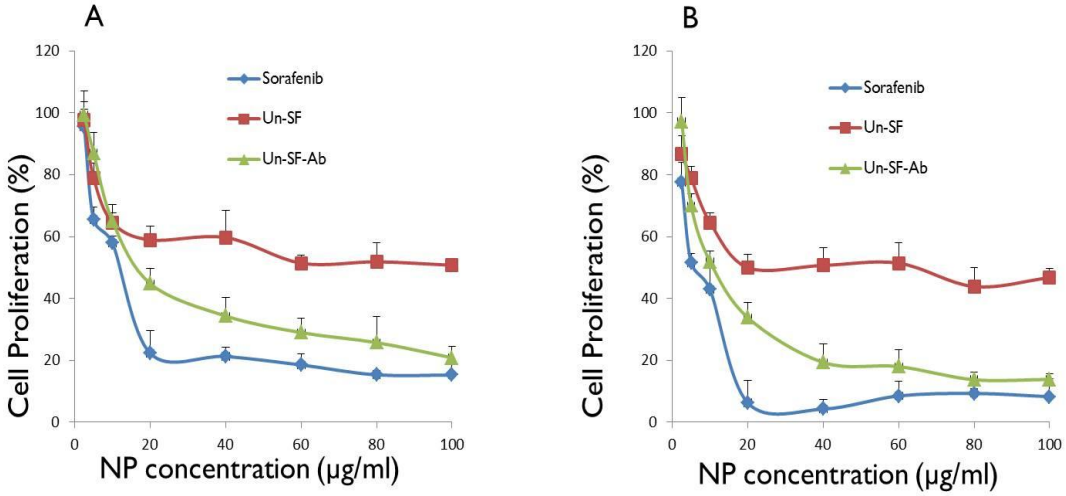

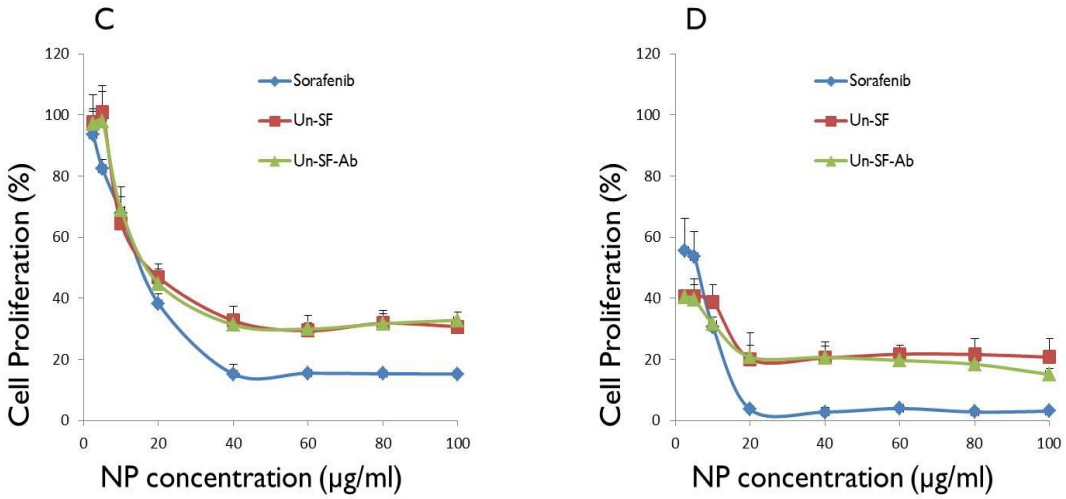

Figure 9. *In vitro anti-proliferation effect of free sorafenib (SF; blue circles), SF-loaded UnTHCPSi (red squares) and SF-loaded anti-EpCAM conjugated UnTHCPSi (green triangles), in MCF-7 (A and B) and MDA-MB-231 (C and D) cells for 24 (A and C) and 48 h (B and D).*

4. Conclusion

Nowadays, one of the biggest concerns in the science world is to develop new and more efficient ways to overcome cancer, as this disease has a high impact in the world population health, being the most lethal. With this in concern, it was mandatory to try and build new systems to avoid some of the anticancer therapy problems as poor solubility of anticancer agents and side effects by lack of cell targeting specificity. In this work, we built a successful targeting system for specific breast cancer cells by biofunctionalization of UnTHCPSi nanoparticles with anti-EpCAM antibody. The NPs with 151± 3.2 nm diameter, which make them suitable to passive targeting by EPR effect, were proven nontoxic in MCF-7 and MDA-MB-231 breast cancer cells until concentrations of 100 µg/mL. The success of the conjugation with the Ab was demonstrated by mean of physicochemical analysis of the conjugate through FTIR spectra, surface charge and size. The use of the PSi NPs also improved the dissolution of sorafenib in human plasma which can lead to the use of smaller drug doses in therapy, avoiding drug resistance by extended exposure to the anticancer agent. Bare NPs had higher dissolution rates than the conjugated, however, the conjugation enhanced the capacity of targeting cells expressing specific antigens, in this case CD326, and

also the intracellular uptake. Thereby, Un-Ab NPs have a higher impact in cell proliferation, being more effective than bare UnTHCPSi NPs in fighting cancer as they are able to deliver the drug to the specific site without interaction with healthy cells, reducing the risk of adverse effects and increasing the drug delivery inside the carcinogenic cells.

Nevertheless, in vitro experiments cannot exactly predict the in vivo behavior of the system. Also, the use of the antibody can improve the anticancer therapy not only by the targeting effect but as well by stimulating the immune system against the tumor tissue. These reasons plus all the advantages of anti-EpCAM UnTHCPSi NPs, as small size, low toxicity, higher dissolution rates, enhanced targeting and intracellular uptake create the need to further research as it is a promising system for breast cancer chemoimmunotherapy with a huge potential for further development.

References

1. Ferlay, J., et al., Estimates of worldwide burden of cancer in 2008: GLOBOCAN 2008. Int J Cancer, 2010. **127**(12): p. 2893-917.

2. Fiandra, L., et al., Assessing the in vivo targeting efficiency of multifunctional nanoconstructs bearing antibody-derived ligands. ACS Nano, 2013. **7**(7): p. 6092-102.

3. World Cancer Report 2014, ed. B.W. Stewart, Wild C. P. 2014: IARC.

4. *http://globocan.iarc.fr*.

5. Alexis, F., et al., Nanoparticle Technologies for Cancer Therapy, in Drug Delivery, M. Schäfer-Korting, Editor. 2010, Springer Berlin Heidelberg. p. 55-86.

6. Zamboni, W.C., et al., Best practices in cancer nanotechnology: perspective from NCI nanotechnology alliance. Clin Cancer Res, 2012. **18**(12): p. 3229-41.

7. Hull, L.C., D. Farrell, and P. Grodzinski, Highlights of recent developments and trends in cancer nanotechnology research-View from NCI Alliance for Nanotechnology in Cancer. Biotechnol Adv, 2013.

8. Mellman, I., G. Coukos, and G. Dranoff, Cancer immunotherapy comes of age. Nature, 2011. **480**(7378): p. 480-489.

9. Moon, J.J., B. Huang, and D.J. Irvine, Engineering nano- and microparticles to tune immunity. Adv Mater, 2012. **24**(28): p. 3724-46.

10. Arruebo, M., M. Valladares, and A. Gonzalez-Fernandez, Antibody-Conjugated Nanoparticles for Biomedical Applications. Journal of Nanomaterials, 2009.

11. Jain, R.K., Transport of Molecules across Tumor Vasculature. Cancer and Metastasis Reviews, 1987. **6**(4): p. 559-593.

12. Weiner, L.M., Monoclonal antibody therapy of cancer. Seminars in Oncology, 1999. **26**(5): p. 43-51.

13. Benet, J.G.-C.a.I., "Tratamiento de los linfomas con anticuerpos monoclonales". Revisiones en Cáncer, 1999. **vol. 13**(no. 4): p. pp. 153-165.

14. Nelson, B., A power surge for cancer immunotherapy. Cancer Cytopathology, 2014. **122**(1): p. 1-2.

15. Secret, E., et al., Antibody-functionalized porous silicon nanoparticles for vectorization of hydrophobic drugs. Adv Healthc Mater, 2013. **2**(5): p. 718-27.

16. The Project on Emerging Nanotechnologies, The Woodrow Wilson International Center for Scholars. http://www.nanotechproject.org, 2008.

17. Mitragotri, S. and J. Lahann, Physical approaches to biomaterial design. Nat Mater, 2009. **8**(1): p. 15-23.

18. Santos, H.A., et al., Mesoporous materials as controlled drug delivery formulations. Journal of Drug Delivery Science and Technology, 2011. **21**(2): p. 139-155.

19. Salonen, J., et al., Mesoporous silicon microparticles for oral drug delivery: loading and release of five model drugs. J Control Release, 2005. **108**(2-3): p. 362-74.

20. Santos, H.A., et al., Multifunctional porous silicon for therapeutic drug delivery and imaging. Curr Drug Discov Technol, 2011. **8**(3): p. 228-49.

21. Salonen, J., et al., Mesoporous silicon in drug delivery applications. J Pharm Sci, 2008. **97**(2): p. 632-53.

22. Boukherroub, R., et al., Thermal Hydrosilylation of Undecylenic Acid with Porous Silicon. Journal of The Electrochemical Society, 2002. **149**(2): p. H59-H63.

23. Rytkonen, J., et al., Functionalization of Mesoporous Silicon Nanoparticles for Targeting and Bioimaging Purposes. Journal of Nanomaterials, 2012.

24. Godin, B., et al., Tailoring the degradation kinetics of mesoporous silicon structures through PEGylation. Journal of Biomedical Materials Research Part A, 2010. **94A**(4): p. 1236-1243.

25. Canham, L.T., Bioactive silicon structure fabrication through nanoetching techniques. Advanced Materials, 1995. **7**(12): p. 1033-&.

26. Helder A. Santos, J.S., Luis M. Bimbo, Porous Silicon for Drug Delivery. Encyclopedia of Metalloproteins, 2013: p. 1773-1781.
27. Koutsopoulos, S., Molecular fabrications of smart nanobiomaterials and applications in personalized medicine. Advanced Drug Delivery Reviews, 2012. **64**(13): p. 1459-1476.
28. Zhang, X.Q., et al., Interactions of nanomaterials and biological systems: Implications to personalized nanomedicine. Advanced Drug Delivery Reviews, 2012. **64**(13): p. 1363-1384.
29. Canham, L.T., Silicon quantum wire array fabrication by electrochemical and chemical dissolution of wafers. Applied Physics Letters, 1990. **57**(10): p. 1046-1048.
30. Jurbergs, D., et al., Silicon nanocrystals with ensemble quantum yields exceeding 60%. Applied Physics Letters, 2006. **88**(23): p. 233116-233116-3.
31. Santos, H.A., Porous Silicon - Revolutionising Drug Targeting and Delivery. NANO MAGAZINE, 2012(24).
32. Hobbs, S.K., et al., Regulation of transport pathways in tumor vessels: role of tumor type and microenvironment. Proc Natl Acad Sci U S A, 1998. **95**(8): p. 4607-12.
33. Zhang, Q., et al., Biocompatible, Uniform, and Redispersible Mesoporous Silica Nanoparticles for Cancer-Targeted Drug Delivery In Vivo. Advanced Functional Materials, 2013: p. n/a-n/a.
34. Gu, L., et al., Multivalent Porous Silicon Nanoparticles Enhance the Immune Activation Potency of Agonistic CD40 Antibody. Advanced Materials, 2012. **24**(29): p. 3981-3987.
35. Savage, D.J., et al., Porous silicon advances in drug delivery and immunotherapy. Curr Opin Pharmacol, 2013. **13**(5): p. 834-41.
36. Fumarola, C., et al., Effects of sorafenib on energy metabolism in breast cancer cells: role of AMPK-mTORC1 signaling. Breast Cancer Res Treat, 2013. **141**(1): p. 67-78.
37. Limnell, T., et al., Surface chemistry and pore size affect carrier properties of mesoporous silicon microparticles. International Journal of Pharmaceutics, 2007. **343**(1-2): p. 141-147.
38. Salonen, J., et al., Stabilization of porous silicon surface by thermal decomposition of acetylene. Applied Surface Science, 2004. **225**(1-4): p. 389-394.
39. Brunauer, S., P.H. Emmett, and E. Teller, Adsorption of Gases in Multimolecular Layers. Journal of the American Chemical Society, 1938. **60**(2): p. 309-319.
40. Santos, H.A., et al., In vitro cytotoxicity of porous silicon microparticles: effect of the particle concentration, surface chemistry and size. Acta Biomater, 2010. **6**(7): p. 2721-31.

41. Danhier, F., O. Feron, and V. Preat, To exploit the tumor microenvironment: Passive and active tumor targeting of nanocarriers for anti-cancer drug delivery. J Control Release, 2010. **148**(2): p. 135-46.

42. *http://www.piercenet.com/method/carbodiimide-crosslinker-chemistry*.

43. Santos, H.A., et al., In vitro cytotoxicity of porous silicon microparticles: Effect of the particle concentration, surface chemistry and size. Acta Biomaterialia, 2010. **6**(7): p. 2721-2731.

44. Bhattacharjee, S., et al., Cytotoxicity of surface-functionalized silicon and germanium nanoparticles: the dominant role of surface charges. Nanoscale, 2013. **5**(11): p. 4870-4883.

45. Crouch, S.P.M., et al., The Use of Atp Bioluminescence as a Measure of Cell-Proliferation and Cytotoxicity. Journal of Immunological Methods, 1993. **160**(1): p. 81-88.

46. Jain, L., et al., Population pharmacokinetic analysis of sorafenib in patients with solid tumours. British Journal of Clinical Pharmacology, 2011. **72**(2): p. 294-305.

47. Krasnici, S., et al., Effect of the surface charge of liposomes on their uptake by angiogenic tumor vessels. International Journal of Cancer, 2003. **105**(4): p. 561-567.

48. Gratton, S.E., et al., The effect of particle design on cellular internalization pathways. Proc Natl Acad Sci U S A, 2008. **105**(33): p. 11613-8.

49. Zhang, H., et al., Diatom silica microparticles for sustained release and permeation enhancement following oral delivery of prednisone and mesalamine. Biomaterials, 2013. **34**(36): p. 9210-9.